Isolation and Structure Elucidation of Kadlongilactones C–F from Kadsura longipedunculata by NMR Spectroscopy and DFT Computational Methods

ARTICLE *in* JOURNAL OF NATURAL PRODUCTS · DECEMBER 2007

Impact Factor: 3.8 · DOI: 10.1021/np070247a · Source: PubMed

11 AUTHORS, INCLUDING:

Jian-Xin Pu
Chinese Academy of Sciences
170 PUBLICATIONS **1,706** CITATIONS
SEE PROFILE

Sheng-Xiong Huang
The Scripps Research Institute
122 PUBLICATIONS **2,179** CITATIONS
SEE PROFILE

Hua-Jie Zhu
Chinese Academy of Sciences
101 PUBLICATIONS **1,089** CITATIONS
SEE PROFILE

Isolation and Structure Elucidation of Kadlongilactones C−F from *Kadsura longipedunculata* by NMR Spectroscopy and DFT Computational Methods

Jian-Xin Pu,[†] Sheng-Xiong Huang,[†] Jie Ren,[†] Wei-Lie Xiao,[†] Li-Mei Li,[†] Rong-Tao Li,[†] Liang-Bo Li,[†] Tou-Gen Liao,[†] Li-Guang Lou,[‡] Hua-Jie Zhu,*[,†] and Han-Dong Sun*[,†]

State Key Laboratory of Phytochemistry and Plant Resources in West China, Kunming Institute of Botany, Chinese Academy of Sciences, Kunming 650204, People's Republic of China, and Shanghai Institute of Materia Medica, Shanghai Institutes for Biological Science, Chinese Academy of Sciences, Shanghai 2000332, People's Republic of China

Received May 26, 2007

Four new triterpenoids, kadlongilactones C−F (**2**−**5**), containing a consecutive hexacyclic [7,7,5,6,6,6] ring system, were isolated from the leaves and stems of *Kadsura longipedunculata*. In comparison with the NMR data of kadlongilactones A (**1**) and D (**3**), a significant phenomena was discovered that ring D of **3** inverted from a half-chair in **1** to a half-boat conformation when the HO-16 group changed from α- to β-orientation. The structures of **2**−**5** were established on the basis of detailed spectroscopic analysis, and DFT computational methods were applied in the structural validation of compounds **3** and **5**. Compounds **1**−**4** showed significant cytotoxicity against A549, HT-29, and K562 cell lines with IC_{50} values of 0.49−3.61 μM *in vitro*.

Recently, the isolation and characterization of some highly oxygenated triterpenoids with unique skeletons from several plants of the genera *Schisandra* and *Kadsura*, which belong to the medicinally important family Schisandraceae, have been reported.[1−7] With the aim of searching for new natural compounds with interesting biological activities, we investigated the leaves and stems of *Kadsura longipedunculata* Finet et Gagnep and reported two novel series of triterpene dilactones with unprecedented rearranged skeletons, named kadlongilactones A and B and longipedlactones A−I, respectively.[8,9] In our continuous investigation of chemically novel and biologically potent active compounds from the same plant, four new compounds, kadlongilactones C−F (**2**−**5**), possessing the same hexacyclic ring system as kadlongilactone A (**1**), were isolated. We report here on the structural elucidation of these new compounds, which are discussed on the basis of their spectroscopic data, specifically those obtained from 2D NMR experiments. In addition, following the encouraging results obtained in the preceding paper concerning the validation of the relative configuration of organic compounds by DFT (density functional theory) calculation methods,[10−15] we considered here the possibility of applying such a method to study the conformation and configuration of two C-16 diastereoisomers (**1** and **3**) and the stereochemical assignment of an epoxide in **5** by a comparison of the experimental ^{13}C NMR chemical shifts with those predicted using DFT computational methods. The cytotoxicity assessment showed that compounds **1**−**4** showed significant activity against three kinds of human tumor cell lines, viz., A549, HT-29, and K562.

Results and Discussion

Kadlongilactone C (**2**) was isolated as a white powder. Its molecular formula of $C_{31}H_{40}O_6$ was established on the basis of negative HRESIMS analysis ($[M - H]^-$, *m/z* 507.2753) and its ^{13}C NMR spectrum, indicating 12 degrees of unsaturation. The IR spectrum showed absorption bands of hydroxy (3432 cm^{-1}) and lactone carbonyl groups (1678 and 1717 cm^{-1}). Its negative FABMS exhibited a peak at *m/z* 490 $[M - H_2O]^-$, further confirming the presence of a hydroxy group. The ^1H NMR (Table 1) spectrum displayed characteristic resonances for four tertiary methyls (δ_H 1.41, 1.43, 1.43, and 1.94), one secondary methyl (δ_H 1.31, J = 6.9 Hz, d), four olefinic protons (δ_H 5.98, 6.24, 6.57, and 6.66), and an *O*-methyl group (δ_H 3.35, s). The ^{13}C NMR (Table 2) and DEPT spectra of **2** showed resonances for 31 carbons: two α,β-unsaturated lactone carbons, seven quaternary carbons (including four olefinic carbons and two oxygenated carbons), 11 methines (four olefinic and two oxygenated), five methylenes, and five methyls (including a secondary methyl), of which 30 were assigned to the triterpene skeleton, and the remaining was ascribed to an *O*-methyl group. Apart from four double bonds and two lactone carbonyl groups, the remaining elements of the unsaturation in **2** were assumed to be a hexacyclic skeleton. Comparison of the ^1H and ^{13}C NMR data for **2** with those of kadlongilactone A (**1**)[8] suggested structural similarities. In fact, most of the NMR data for **2** resembled those of **1**. The main differences between the ^{13}C NMR spectra of **2** and **1** were the presence of an *O*-methyl group (δ_C 56.1) and the chemical shift of C-15 and C-16 in **2**. The HMBC correlations from OCH_3 to C-16, as well as the $^1H-^1H$ COSY spin system H-16/H_2-15, confirmed the location of OCH_3 at C-16. H-16 (δ_H 3.84, $\Delta\delta_{1,2}$ = 0.80 ppm) resonated at a higher field than the comparable signal in **1** (δ_H 4.64) due to the weaker deshielding effect of OCH_3 in **2**.

The relative configuration of the stereocenters of **2** were assigned as the same as those of **1** on the basis of the similarity of all the proton and carbon chemical shifts and proton multiplicities for both compounds. In the ROESY spectrum of **2**, H-16 showed correlations with H-15α, H-15 β, H-20α, and H_3-21 like those of **1** in Figure 2, indicating that CH_3O-16 should be α-oriented. Therefore, it was suggested that **2** was 16α-*O*-methylkadlongilactone A and named kadlongilactone C.

The composition of kadlongilactone D (**3**) was found to be $C_{30}H_{38}O_6$ (12 degrees of unsaturation) by its negative HRESIMS (*m/z* 493.2591 $[M - H]^-$) and NMR data. Comparison of NMR data of **3** with those of **1** revealed similar structures for rings A, B, and F. However, the data for the remaining portion of the structure of **3** were different from those of **1**. The C-11, C-13, C-14, C-16, C-20, and C-28 resonances were shifted downfield from δ_C 49.2, 133.2, 40.9, 64.1, 34.4, and 27.4 ppm in **1** to δ_C 51.9, 136.4, 42.5, 67.0, 37.3, and 30.0 ppm in **3**, respectively, and the C-8, C-15, and C-17 resonances were shifted upfield from δ_C 56.0, 45.7, and 131.3 in **1** to δ_C 54.5, 44.0, and 130.2 in **3**. In support of these differences, we postulate that the HO-16 orientation changed from α in **1** to β in **3** and that the half-chair conformation of ring D in **1** was converted to the half-boat conformation in **3**.

* Corresponding author. Phone: (86) 871-5223251. Fax: (86) 871-5216343. E-mail: hjzhu@mail.kib.ac.cn; hdsun@mail.kib.ac.cn.
[†] Kunming Institute of Botany.
[‡] Shanghai Institute of Materia Medica.

10.1021/np070247a CCC: $37.00
Published on Web 10/31/2007

Table 1. ^{1}H NMR Assignments of Compounds **1**–**5**[a]

proton	1	2	3	4	5
1	6.53 (d, 12.2)	6.57 (d, 12.2)	6.38 (d, 12.2)	6.43 (d, 12.3)	6.54 (d, 12.6)
2	5.96 (d, 12.2)	5.98 (d, 12.2)	5.92 (d, 12.2)	5.95 (d, 12.3)	5.92 (d, 12.6)
5	4.09 (d, 9.3)	4.11 (d, 9.3)	4.02 (d, 9.4)	4.02 (d, 9.3)	4.03 (d, 9.9)
6α	2.16 (m)	2.24 (overlap)	2.20 (overlap)	2.28 (overlap)	2.07 (m)
6*β*	1.25 (m)	1.27 (overlap)	1.20 (m)	1.22 (overlap)	1.09 (m)
7α	2.31 (overlap)	2.31 (overlap)	2.28 (overlap)	2.25 (overlap)	2.19 (m)
7*β*	1.78 (m)	1.79 (m)	1.84 (overlap)	1.85 (m)	1.55 (overlap)
8	1.63 (dd, 2.0, 12.7)	1.51 (overlap)	1.59 (dd, 1.8, 11.9)	2.36 (overlap)	1.47 (overlap)
11α	2.47 (dd, 7.4, 13.2)	2.33 (overlap)	2.54 (overlap)	2.57 (overlap)	2.40 (dd, 7.5, 14.3)
11*β*	1.37 (overlap)	1.25 (overlap)	1.87 (overlap)	1.63 (m)	2.70 (dd, 9.6, 14.3)
12	2.70 (m)	2.67 (m)	2.58 (overlap)	2.70 (m)	2.90 (dd, 7.5, 9.6)
15α	1.93 (overlap)	1.47 (overlap)	1.34 (overlap)	0.94 (dd, 2.5, 15.1)	1.69 (d, 15.1)
15*β*	1.93 (overlap)	2.01 (m)	2.23 (overlap)	2.20 (dd, 2.5, 15.1)	1.95 (dd, 3.8, 15.1)
16	4.64 (brs)	3.84 (s)	4.48 (brs)	3.53 (s)	3.50 (d, 3.8)
18α	1.98 (overlap)	1.96 (overlap)	2.02 (dd, 6.3, 17.1)	1.98 (overlap)	2.32 (dd, 4.4, 13.2)
18*β*	2.06 (m)		2.12 (m)	2.06 (m)	1.51 (overlap)
19	6.22 (s)	6.24 (s)	6.02 (s)	6.03 (s)	6.50 (s)
20	3.23 (m)	2.94 (brs)	2.67 (brs)	2.53 (overlap)	3.28 (m)
21	1.57 (d, 7.3)	1.31 (d, 6.9)	1.58 (d, 7.2)	1.33 (d, 7.3)	1.00 (d, 7.2)
22	4.48 (dd, 2.0, 4.4)	4.42 (brs)	4.45 (m)	4.40 (brs)	4.52 (s)
23	2.26 (overlap)	2.29 (overlap)	2.38 (m)	2.34 (overlap)	3.10 (m)
24	6.71 (dd, 1.5, 6.4)	6.66 (d, 6.4)	6.74 (dd, 1.4, 6.3)	6.72 (d, 6.4)	6.64 (dd, 6.1)
27	1.95 (s)	1.94 (s)	1.96 (s)	1.93 (s)	1.86 (s)
28	1.54 (s)	1.43 (s)	1.31 (s)	1.30 (s)	1.57 (s)
29	1.43 (s)	1.43 (s)	1.42 (s)	1.44 (s)	1.42 (s)
30	1.41 (s)	1.41 (s)	1.39 (s)	1.43 (s)	1.38 (s)
9-OH	6.53 (s)	6.51 (s)	6.33 (s)	6.45 (s)	6.52 (s)
16-OH					6.60 (s)
16-OCH_3		3.35 (s)		3.12 (s)	

[a] Data were recorded in C_5D_5N on a Bruker DRX (^{1}H, 400 MHz); chemical shifts (*δ*) are expressed in ppm with reference to the most downfield signal of C_5D_5N (*δ* 8.71 ppm) for ^{1}H.

Table 2. ^{13}C NMR Assignments of Kadlongilactones C−F (**1**–**5**)[a]

carbon	1	2	3	4	5
1	144.2 (d)	144.0 (d)	144.3 (d)	144.2 (d)	144.2 (d)
2	119.2 (d)	119.2 (d)	119.0 (d)	119.1 (d)	119.2 (d)
3	166.5 (s)	166.5 (s)	166.6 (s)	166.6 (s)	166.5 (s)
4	80.3 (s)	80.1 (s)	80.2 (s)	80.2 (s)	80.3 (s)
5	48.5 (d)	48.5 (d)	48.7 (d)	48.8 (d)	48.2 (d)
6	28.4 (t)	28.5 (t)	28.5 (t)	28.1 (t)	27.9 (t)
7	27.8 (t)	27.9 (t)	27.4 (t)	27.5 (t)	27.3 (t)
8	56.0 (d)	57.7 (d)	54.5 (d)	53.8 (d)	58.8 (d)
9	79.1 (s)	78.8 (s)	79.7 (s)	79.6 (s)	79.3 (s)
10	145.6 (s)	145.7 (s)	145.3 (s)	145.9 (s)	145.6 (s)
11	49.2 (t)	47.4 (t)	51.9 (t)	52.3 (t)	44.4 (t)
12	51.0 (d)	50.8 (d)	51.1 (d)	50.6 (d)	53.0 (d)
13	133.2 (s)	134.0 (s)	136.4 (s)	137.8 (s)	74.0 (s)
14	40.9 (s)	40.0 (s)	42.5 (s)	42.4 (s)	43.6 (s)
15	45.7 (t)	37.7 (t)	44.0 (t)	35.4 (t)	36.0 (t)
16	64.1 (d)	73.8 (s)	67.0 (s)	76.8 (d)	54.3 (d)
17	131.3 (s)	128.4 (s)	130.2 (s)	127.8 (s)	63.6 (s)
18	32.1 (t)	32.1 (t)	32.9 (t)	32.6 (t)	35.1 (t)
19	148.2 (d)	147.7 (d)	148.4 (d)	148.4 (d)	149.6 (d)
20	34.4 (d)	34.2 (d)	37.3 (d)	37.0 (d)	32.6 (d)
21	14.7 (q)	14.7 (q)	14.6 (q)	14.0 (q)	8.8 (q)
22	80.1 (d)	79.9 (d)	79.8 (d)	79.5 (d)	81.4 (d)
23	33.3 (d)	33.0 (d)	33.3 (d)	33.2 (d)	33.2 (d)
24	146.1 (d)	145.9 (d)	146.0 (d)	145.9 (d)	145.0 (d)
25	127.9 (s)	127.8 (s)	127.8 (s)	127.7 (s)	128.1 (s)
26	166.7 (s)	166.6 (s)	166.6 (s)	166.6 (s)	166.1 (s)
27	17.2 (q)	17.1 (q)	17.2 (q)	17.1 (q)	17.3 (q)
28	27.4 (q)	25.8 (q)	30.0 (q)	29.9 (q)	28.9 (q)
29	25.8 (q)	25.7 (q)	25.7 (q)	25.8 (q)	25.8 (q)
30	29.4 (q)	29.3 (q)	29.3 (q)	29.4 (q)	29.4 (q)
16-OCH_3		56.1		55.2	

[a] Data were recorded in C_5D_5N on a Bruker DRX (^{13}C, 100 MHz); chemical shifts (*δ*) are expressed in ppm with reference to the center peak of the most downfield signal of C_5D_5N (*δ* 149.9 ppm) for ^{13}C.

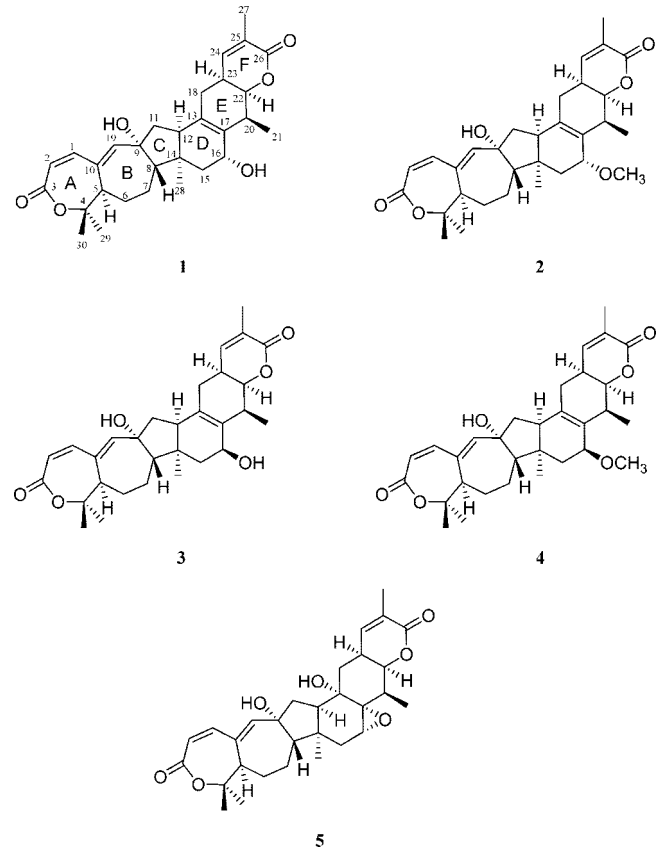

Figure 1. Structures of kadlongilactones C−F (**1**–**5**).

This assignment was further confirmed by a ROESY (Figure 2) experiment. ROESY correlations observed between H-16 and H-20α as well as H_3-21*β*, and between H-16 and H-15α and H-15*β*, in **1** determined the α-orientation of HO-16 and the half-chair conformation of ring D, which was unambiguously determined by X-ray crystallographic analysis.[8] However, the same significant ROESY correlations were also observed from H-16 to H-20α and

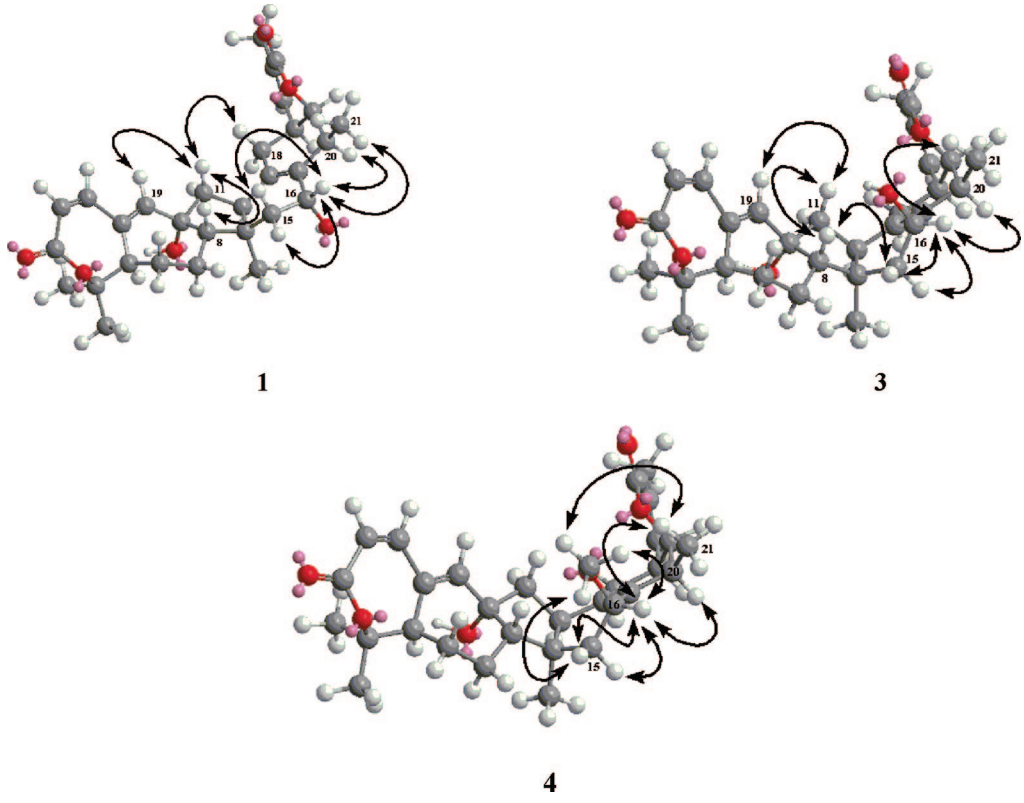

Figure 2. Key ROESY correlations of compounds **1**, **3**, and **4**.

H_3-21β as well as from H-16 to H-15α and H-15β in **3**. The above correlations and the distinct chemical shift differences of vicinal carbons of ring D indicated that the HO-16 transformed from the α-orientation in **1** to β-orientation in **3**, and ring D inverted from the half-chair in **1** to the half-boat in **3**.

The above NMR experiments indicated the possibility of the conformational inversion of ring D. In order to confirm this phenomena, DFT computational studies were performed for **1** and **3**. Optimization was performed at the B3LYP/6-31G* level using the crystal geometry. Two pairs of conformations, **1a** and **1b**/**3a** and **3b**, were found for **1** and **3**, respectively, when ring D was in half-boat (**1a** and **3a**) and half-chair (**1b** and **3b**) conformations. Two conformations, **1a** and **1b**, had a 0.113 kcal/mol energy difference in free energy, and this resulted in 45% and 55% distribution in solution, respectively. However, two conformations for **3** just had a 3.979 kcal/mol difference in free energy, and only one major conformation (**3a**, >98.2%) for **3** existed in solution (Figure 3).

Transition state (TS) computation was performed for conversion between **1a** and **1b** at the B3LYP/6-31G* level again. The energy barrier calculated was 7.1 kcal/mol in free energy from **1b** to **1a**. This barrier was sufficiently low to permit the conversion of **1a** to **1b**, or reverse, at room temperature. This fast conversion between two rigid conformations would affect the observed ^{13}C NMR chemical shifts. Thus, the observed chemical shifts of **1** could be the averaged magnitudes of **1a** and **1b** based on their different distributions. Computations of ^{13}C NMR data for **1a**, **1b**, and **3a** were carried out using three methods, and the calculated magnetic shielding values have been converted into chemical shifts for ready comparison (see Supporting Information).

Table 3 listed the differences between compounds **1** and **3**. Due to the fact that **1a** and **1b** had almost the same distribution (45% vs 55%), and method B gave closer chemical shifts to the experimental values, the average calculated ^{13}C NMR values of **1a** and **1b** obtained by method B were applied in the following analysis.

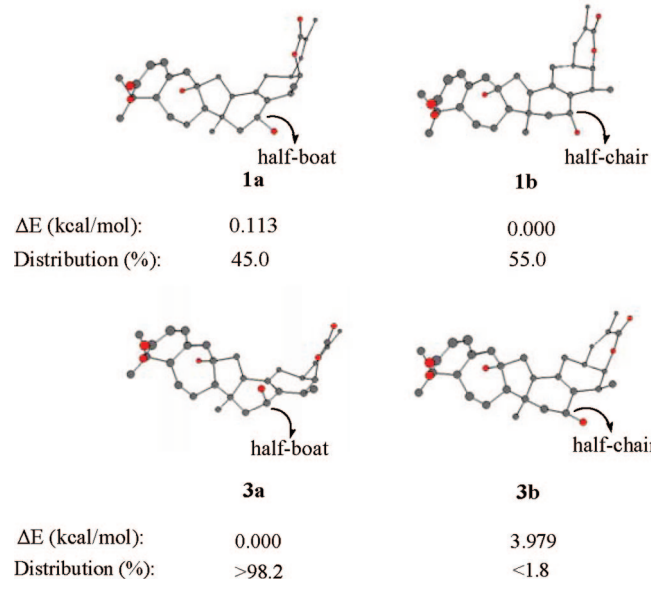

Figure 3. Energy difference and distribution in solution of compounds **1a**,**b** and **3a**,**b**.

In our previous report, empirical corrections were used in computed ^{13}C NMR data for vibralactone, an unusual fused β-lactone, where the slope and intercept of linear-squares correlation lines were selected as reported.[16] This method was also used in this study, and these corrected chemical shifts and the differences between **1** and **3** are summarized in Table 4.

Both the uncorrected and corrected ^{13}C NMR data gave reasonable explanations for the experimental ^{13}C NMR data of **1**. The computational results of **3a** and chemical shift differences, $\Delta\delta$[(**1a** + **1b**)/**2** − **3a**], were in good agreement with the experimental data of **3** and chemical shift differences, $\Delta\delta$(**1**−**3**), respectively. These calculated results further confirmed the relative stereochemical

Table 3. Experimental and Computed Chemical Shift Differences

	$\Delta\delta$ (**1**−**3**)	$\Delta\delta$(**1a**−**3a**)/$\Delta\delta$(**1b**−**3a**)			
carbon number	expt[a]	method A[b]	method B[c]	method C[d]	$\Delta\delta$[(**1a** + **1b**)/**2** − **3a**]
C-1	−0.1	−0.7/−0.6	−0.5/−0.4	−0.5/−0.7	−0.5
C-2	+0.2	+1.2/+1.4	+0.8/+1.1	+0.6/+0.7	+1.0
C-3	−0.1	−0.4/−0.4	−0.3/−0.5	−0.2/−0.3	−0.4
C-4	+0.1	+0.7/+0.2	+0.6/−0.7	0/0	+0.1
C-5	−0.2	−1.5/−0.1	−1.0/+0.9	0/−0.1	−0.1
C-6	−0.1	−1.2/−0.2	−0.6/0	−0.1/0	−0.3
C-7	+0.4	+0.4/+0.6	+0.3/+0.8	0/+0.2	+0.6
C-8	+1.5	−2.7/+4.7	−1.7/+4.5	−0.7/+5.1	+1.4
C-9	−0.6	−0.3/−0.4	−0.4/−0.4	−0.5/−0.4	−0.4
C-10	+0.3	+0.4/+1.2	+0.5/+1.5	+0.7/+1.1	+1.0
C-11	−2.7	+1.3/−6.6	+1.2/−6.0	+1.4/−5.3	−2.4
C-12	−0.1	−0.8/−0.4	−0.7/−0.3	−0.9/−0.9	−0.5
C-13	−3.2	−4.9/−8.1	−4.1/−7.2	−5.0/−8.1	−5.7
C-14	−1.6	−0.8/−3.4	−0.9/−3.3	−0.9/−2.3	−2.1
C-15	+1.7	+5.0/+2.9	+5.6/+2.6	+4.2/+1.8	+4.1
C-16	−2.9	−3.6/−4.5	−3.7/−4.2	−3.0/−2.8	−4.0
C-17	+1.1	−2.7/+0.4	−2.0/−0.1	+3.7/+0.5	−1.1
C-18	−0.8	−0.8/−0.4	−0.5/−0.4	−0.6/−0.3	−0.5
C-19	−0.2	−0.2/−0.7	−0.7/−0.8	−0.9/−1.2	−0.8
C-20	−2.9	−2.2/−1.2	−2.4/−1.4	−2.6/−2.1	−1.9
C-21	+0.1	+0.5/+0.5	+0.4/+0.5	+0.7/+0.7	+0.5
C-22	+0.3	+0.1/−0.2	+0.2/−0.3	+0.5/+1.0	−0.1
C-23	0	−0.6/−1.1	−0.4/−1.2	−0.1/−0.3	−0.8
C-24	+0.1	+0.5/+0.4	+0.4/+0.5	0/−0.2	+0.5
C-25	+0.1	−0.2/−0.3	−0.7/−0.3	+0.2/+0.3	−0.5
C-26	+0.1	+0.2/−0.5	+0.4/−0.4	+0.5/+0.1	0
C-27	0	−0.3/−0.2	−0.4/−0.1	0/+0.1	−0.3
C-28	−2.6	−0.5/−3.3	+0.1/−3.8	−0.4/−3.9	−1.9
C-29	+0.1	0/0	0/−0.1	−0.1/0	−0.1
C-30	+0.1	−0.3/−0.5	−0.2/−0.3	0/0	−0.3

[a] Data were recorded in C_5D_5N on a Bruker DRX (^{13}C, 100 MHz); chemical shifts (δ) are expressed in ppm with reference to the center peak of the most downfield signal of C_5D_5N (δ 149.9 ppm) for ^{13}C. [b] B3LYP/6-311+G(2d,p)//B3LYP/6-31G(d). [c] B3LYP/6-311+G(2d,p)//HF/6-31G(d). [d] HF/6-31G(d)//HF/6-31G(d).

Table 4. Corrected Chemical Shifts and the Differences between **1** and **3**

	corrected chemical shifts (**1a/1b/3a**)			$\Delta\delta$[(**1a** + **1b**)/**2** − **3a**]	$\Delta\delta$(**1**–**3**)
carbon number	method A[b]	method B[c]	method C[d]	method A/B/C	expt[a]
C-1	139.9/140.0/140.1	142.0/142.1/142.7	146.3/146.9/146.8	−0.2/−0.7/0.2	−0.1
C-2	122.2/122.5/120.7	124.3/124.7/123.8	124.5/125.3/124.0	1.7/0.7/0.9	+0.2
C-3	161.9/161.9/161.7	158.6/158.3/158.9	161.6/162.4/161.8	0.2/−0.5/0.2	−0.1
C-4	78.8/78.6/78.1	77.3/76.3/77.3	71.6/72.1/71.9	0.6/−0.5/0.1	0.1
C-5	47.4/49.0/49.0	48.3/50.5/50.1	44.8/45.0/45.1	−0.8/−0.7/−0.2	−0.2
C-6	28.2/29.4/29.5	28.2/29.2/29.8	29.4/29.8/29.8	−0.7/−1.1/−0.2	−0.1
C-7	27.6/28.1/27.4	27.0/28.0/27.7	28.3/28.8/28.7	0.5/−0.2/−0.2	+0.4
C-8	52.0/59.4/54.6	53.3/59.8/55.8	49.7/56.0/50.8	1.1/0.8/2.1	+1.5
C-9	82.4/82.5/82.6	81.1/81.4/82.1	74.3/74.9/75.0	−0.2/−0.9/−0.4	−0.6
C-10	151.3/152.1/150.4	151.9/152.9/151.5	149.3/148.3/148.7	1.3/0.9/0.1	+0.3
C-11	54.1/46.7/52.9	54.1/47.4/53.7	52.7/46.3/51.6	−2.5/−3.0/−2.1	−2.7
C-12	52.0/52.7/52.9	52.3/53.1/53.8	47.8/48.2/49.1	−0.6/−1.1/−1.1	−0.1
C-13	137.2/134.1/141.4	138.1/135.1/142.3	137.1/134.8/142.3	−5.8/−5.7/−6.4	−3.2
C-14	44.3/42.1/45.2	44.1/42.2/45.9	37.7/36.6/38.9	−2.0/−2.8/−1.8	−1.6
C-15	45.6/43.8/40.9	46.9/44.4/42.3	45.9/43.8/42.0	3.8/3.4/2.9	1.7
C-16	66.5/65.8/69.9	65.2/65.1/69.6	61.6/62.3/64.9	−3.8/−4.5/−3.0	−2.9
C-17	133.2/136.3/135.4	135.0/136.9/137.2	137.3/134.9/133.7	−0.7/−1.3/2.4	1.1
C-18	33.3/34.0/34.2	33.1/33.6/34.5	34.4/35.1/35.4	−0.6/−1.2/−0.7	−0.8
C-19	144.1/143.7/143.8	144.3/144.2/145.1	144.8/145.4/145.8	0.1/−0.9/−0.7	−0.2
C-20	35.8/37.1/38.1	35.8/37.2/39.1	34.4/35.3/37.4	−1.7/−2.6/−2.6	−2.9
C-21	12.5/12.8/12.3	11.8/12.4/12.5	19.0/19.3/18.7	0.4/−0.4/0.5	+0.1
C-22	78.4/78.4/78.3	77.0/76.8/77.4	72.1/73.2/71.9	0.1/−0.5/0.8	+0.3
C-23	34.7/34.6/35.5	34.7/34.3/36.0	33.3/33.4/33.8	−0.9/−1.5/−0.5	0
C-24	143.3/143.3/142.4	143.7/143.8/143.5	147.9/148.5/148.0	0.9/0.3/0.2	+0.1
C-25	131.9/131.9/131.7	132.9/133.4/133.9	131.2/132.0/131.1	0.2/−0.8/0.5	+0.1
C-26	163.5/162.8/162.7	160.6/159.8/160.3	162.7/163.2/162.2	0.5/−0.1/0.8	+0.1
C-27	16.8/17.3/17.4	16.4/17.3/17.9	21.8/22.1/22.2	−0.3/−1.1/−0.3	0
C-28	26.5/24.1/27.2	27.1/23.7/28.0	31.6/28.3/32.4	−1.9/−2.6/−2.5	−2.6
C-29	22.6/23.0/22.9	22.8/23.1/23.8	28.5/29.0/29.0	−0.1/−0.9/−0.3	+0.1
C-30	26.1/26.3/26.7	26.7/27.1/27.9	32.5/32.8/32.9	−0.5/−1.0/−0.3	+0.1

[a] Data were recorded in C_5D_5N on a Bruker DRX (^{13}C, 100 MHz); chemical shifts (δ) are expressed in ppm with reference to the center peak of the most downfield signal of C_5D_5N (δ 149.9 ppm) for ^{13}C. [b] B3LYP/6-311+G(2d,p)//B3LYP/6-31G(d). [c] B3LYP /6-311+ G(2d,p)//HF/6-31G(d). [d] HF/6-31G(d)//HF/6-31G(d).

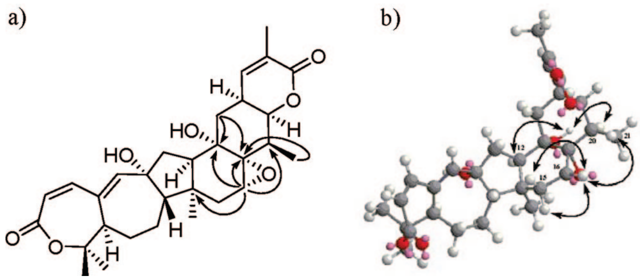

Figure 4. (a) Key HMBC (H→C) correlations of **5**; (b) key ROESY (↔) correlations of **5**.

correctness of **3**, whose ring D reversed from half-chair conformation in **1** to half-boat. Therefore, through the above NMR and DFT analyses, the structure of **3** was unambiguously determined as showed in Figure 1 and named kadlongilactone D.

Kadlongilactone E (**4**) was obtained as a white powder with the empirical formula $C_{31}H_{40}O_6$, in agreement with the HRESIMS (*m/z* 507.2741 $[M - H]^-$, calcd for $C_{31}H_{39}O_6$, 507.2746) and ^{13}C NMR data. The NMR data of **4** were similar to those of **3**. The only difference was that the NMR spectra of **4** displayed resonances due to an *O*-methyl group (δ_H 3.12, δ_C 55.2), where the *O*-methyl protons were correlated with C-16 (δ_C 76.8) in the HMBC spectrum, demonstrating the C-16 location of the *O*-methyl group. In the ROESY (Figure 2) spectrum, CH_3O-16 had correlations with H-15β and H-21β, indicating CH_3O-16 to be β-oriented, and correlations between H-16/H-15α, H-16/H-15β, H-16/H-20, and H-16/H_3-21 in **4**, indicating ring D adopted a half-boat conformation. Thus, the structure of **4** was determined to be 16-epikadlongilactone C and named kadlongilactone E.

Kadlongilactone F (**5**) was obtained as a white powder. The $[M - H]^-$ ion peak at *m/z* 509.2529 (calcd for $C_{30}H_{37}O_7$, 509.2539) in the HRESIMS determined its molecular formula to be $C_{30}H_{38}O_7$, differing from **1** by the addition of an oxygen atom. Detailed comparison of ^1H and ^{13}C NMR data of **5** with those of **1** showed close analogy. The major differences included the appearance of a trisubstituted epoxide with an α-hydroxy carbon in **5** and the disappearance of a double bond (δ_C 131.3, s and 133.2, s) in **1**. Considering the chemical shifts [74.0 (s, C-13), 54.3 (d, C-16), and 63.6 (s, C-17)], the 13-hydroxy-16,17-epoxide moiety was the most appropriate structure.[17] The HMBC (Figure 4a) correlations of H-16 (δ_H 3.50, d, $J = 3.9$ Hz) to C-13, C-14, C-17, and C-20; H_3-21 to C-17; and H_2-18 to C-13 and C-17 further verified that the epoxide group was positioned between C-16 and C-17. In the ROESY (Figure 4b) experiment, H-16 showed strong correlations with H-15α, H-15β, and H_3-21β and lack of correlation with H-20α, together with a scalar coupling of only 3.8 Hz between H-16 and H-15β, indicating an α-orientation of the epoxide group. HO-16 (δ_H 6.60, s) showed correlations with H-12α and H-20α, indicating its α-orientation. To support this stereochemical assignment, DFT caculations were employed again via methods A, B, and C in ^{13}C NMR data computations of **5**. The computed results (see Supporting Information) of **5** agreed well with the experimental results. Thus, all of these data confirmed the structure for **5** with an epoxide of α-orientation located between C-16 and C-17.

The *in vitro* cytotoxicity of compounds **1–4** was evaluated against three kinds of human tumor cell lines (A549, HT-29, and K562). Compounds **1–4** showed cytotoxicity against all three cell lines with IC_{50} values of 0.49–3.61 μ M, and **3** exhibited the most potent cytotoxicity, with IC_{50} values of 0.49 (A549), 1.64 (HT-29), and 1.92 (K562) μM, respectively (Table 5). Because of the small quantity of compound **5**, its cytotoxicity was not tested.

Table 5. Cytotoxic Activities of Compounds **1–4** against Tumor Cell Lines

compd	IC_{50} (μM) A 549	HT-29	K562
1	1.24	1.44	3.44
2	1.45	2.08	3.61
3	0.49	1.64	1.92
4	0.88	1.32	3.35
positive control amrubicin hydrochloride	0.82	4.36	1.26

Experimental Section

General Experimental Procedures. Optical rotations were measured on a JASCO DIP-370 digital polarimeter. IR spectra were obtained on a Bio-Rad FtS-135 spectrophotometer with KBr pellets, whereas UV data were obtained using a UV-210A spectrometer. MS were recorded on a VG Auto Spec-3000 spectrometer. 1D NMR spectra were obtained on a Bruker DRX-400 instrument with TMS as an internal standard, and 2D NMR spectra were obtained on a Bruker DRX-500 instrument with TMS as an internal standard. Column chromatography (CC) and TLC: Si gel (200–300 mesh) from Qingdao Marine Chemical Factory, Quingdao, People's Republic of China.

Plant Material. The leaves and stems of *K. longipedunculata* were collected in Erlang mountain region of Sichuan Province, China, in August 2004, and identified by Prof. Xi-Wen Li, Kunming Institute of Botany. A voucher specimen has been deposited in the Herbarium of the Kunming Institute of Botany, Chinese Academy of Sciences.

Extraction and Isolation. The air-dried and powdered stems (11 kg) of *K. longipedunculata* were extracted with 70% aqueous Me_2CO (3 × 30 L) at room temperature to yield an extract, which was successively extracted with petroleum ether and EtOAc. The EtOAc extract was evaporated to dryness under reduced pressure to give an extract (300 g) that was separated by Si gel CC (1.5 kg, 200–300 mesh) and eluted with a $CHCl_3/Me_2CO$ gradient system (9:1, 8:2, 7:3, 6:4, 5:5) to give fractions 1–5. Fractions 1 (40 g) and 2 (15 g) were subjected to CC with $CHCl_3/(CH_3)_2CHOH$ (30:1) to afford seven and five fractions, respectively, which were further purified by semipreparative HPLC (Agilent 1100 HPLC system, U.S.A; Zorbax SB-C-18, Agilent, 9.4 mm × 25 cm, U.S.A., $MeOH/H_2O$) to give compounds **2** (4.1 mg), **3** (11.2 mg), and **4** (4.3 mg). Fraction 3 (30 g) was subjected to CC with $CHCl_3/CH_3OH$ (20:1) to afford six fractions, which were further purified by Sephadex LH-20 (CH_3OH) to afford another seven fractions, and fraction 2 was purified by semipreparative HPLC ($MeOH/H_2O$) to give compound **5** (1.4 mg).

Kadlongilactone C (2): white powder; $[\alpha]_D^{26.9}$ −108.9 (*c* 0.22, C_5H_5N); UV (MeOH): λ_{max} (log ε) 279 (4.59), 203 (4.62) nm; IR (KBr) υ_{max} 3432, 2926, 2878, 1717, 1678, 1129, 1076 cm^{-1}; negative FABMS *m/z* 599 $[M + Gly - H]^-$, 507 $[M - H]^-$, 490 $[M - H_2O]^-$; positive HRESIMS *m/z* 507.2753 [calcd for $C_{31}H_{40}O_6$ $(M - H)^-$, 507.2746]; ^1H and ^{13}CNMR data (Tables 1 and 2).

Kadlongilactone D (3): white powder; $[\alpha]_D^{25.1}$ –207.7 (*c* 4.68, C_5H_5N); UV (MeOH) λ_{max} (log ε) 344 (2.84), 279 (4.48), 205 (4.53) nm; IR (KBr) υ_{max} 3444, 2925, 1700, 1672, 1132 cm^{-1}; negative FABMS *m/z* 585 $[M + Gly - H]^-$, 493 $[M - H]^-$· 476 $[M - H_2O]^-$; positive HRESIMS *m/z* 493.2591 [calcd for $C_{30}H_{38}O_6$ $(M - H)^-$, 493.2590]; ^1H and ^{13}CNMR data (Tables 1 and 2).

Kadlongilactone E (4): white powder; $[\alpha]_D^{25}$ –196.6 (*c* 1.30, C_5H_5N); UV (MeOH): λ_{max} (log ε) 352 (2.75), 279 (4.56), 206 (4.68) nm; IR (KBr) υ_{max} 3440, 2926, 2858, 1692, 1676, 1644, 1130 cm^{-1}; negative FABMS *m/z* 599 $[M + Gly - H]^-$, 507 $[M - H]^-$, 490 $[M - H_2O]^-$; positive HRESIMS *m/z* 507.2741 [calcd for $C_{31}H_{40}O_6$ $(M - H)^-$, 507.2746]; ^1H and ^{13}CNMR data (Tables 1 and 2).

Kadlongilactone F (5): white powder; $[\alpha]_D^{20.0}$ +121.5 (*c* 0.85, C_5H_5N); UV (MeOH) λ_{max} (log ε) 279 (4.60), 217 (4.37), 200 (4.41) nm; IR (KBr) υ_{max} 3478, 3427, 2962, 2926, 2940, 2882, 1705, 1679, 1141, 1119 cm^{-1}; negative FABMS *m/z* 693 $[M + 2Gly - H]^-$, 601 $[M + Gly H]^-$, 509 $[M - H]^-$; positive HRESI MS *m/z* 509.2529 [calcd for $C_{30}H_{37}O_7$ $(M - H)^-$, 509.2539]; ^1H and ^{13}CNMR data (Tables 1 and 2).

Computational Methods. Optimizations were performed using the Gaussian 03 program.[18] Method A: The structures were optimized at the B3LYP/6-31G* level of theory, and their ^{13}C NMR spectra were then obtained at the 6-311+G(2d,p) level of theory (B3LYP/6-311+G(2d,p)//B3LYP/6-31G*). Method B: The structures were optimized at the HF/6-31G* level of theory, and their ^{13}C NMR spectra were then obtained at the DFT/6-311+G(2d,p) level of theory (B3LYP/6-311+G(2d,p)//HF/6-31G*). Method C: The structures were optimized

at the HF/6-31G* level of theory, and their ^{13}C NMR spectra were then obtained at the HF/6-31G* level of theory (HF/6-31G*//HF/6-31G*).

Cytotoxicity Bioassays. Cytotoxicity of compounds against suspended tumor cells was determined by the trypan blue exclusion method. Cytotoxicity against adherent cells was determined by a sulforhodamine B (SRB) assay. Cells were plated in 96-well plates 24 h before treatment and continuously exposed to different concentrations of compounds for 72 h. After compound treatment, cells were counted (suspended cells) or fixed and stained with SRB (adherent cells) as described.[19]

Acknowledgment. We gratefully acknowledge the support of the Yong Academic and Technical Leader Raising Foundation of Yunnan Province (2006PY01-47), the Natural Science Foundation of Yunnan Province (2005XY04 and 2006B0042Q), the National Natural Science Foundation of China (20402016), fund of CAS (YZ-06-01), and the key Scientific and Technological Projects of Yunnan Province (2004NG12, 2005B0048M).

Supporting Information Available: ^{1}H, ^{13}C NMR spectra, MS data, 2D NMR spectra of kadlongilactones C−F (**2**–**5**), and computed data using the DFT method. This material is available free of charge via the Internet at http://pubs.acs.org.

References and Notes

(1) Li, R. T.; Zhao, Q. S.; Li, S. H.; Han, Q. B.; Sun, H. D.; Lu, Y.; Zhang, L. L.; Zheng, Q. T. *Org. Lett.* **2003**, *5*, 1023–1026.
(2) Li, R. T.; Xiao, W. L.; Shen, Y. H.; Zhao, Q. S.; Sun, H. D. *Chem.−Eur. J.* **2005**, *11*, 2989–2996.
(3) Xiao, W. L.; Li, R. T.; Li, S. H.; Li, X. L.; Sun, H. D.; Zheng, Y. T.; Wang, R. R.; Lu, Y.; Wang, C.; Zheng, Q. T. *Org. Lett.* **2005**, *7*, 1263–1266.
(4) Xiao, W. L.; Zhu, H. J.; Shen, Y. H.; Li, R. T.; Li, S. H.; Sun, H. D.; Zheng, Y. T.; Wang, R. R.; Lu, Y.; Wang, C.; Zheng, Q. T. *Org. Lett.* **2005**, *7*, 2145–2148.
(5) Xiao, W. L.; Pu, J. X.; Chang, Y.; Li, X. L.; Huang, S. X.; Yang, L. M.; Li, L. M.; Lu, Y.; Zheng, Y. T.; Li, R. T.; Zheng, Q. T.; Sun, H. D. *Org. Lett.* **2006**, *8*, 1475–1478.
(6) Xiao, W. L.; Yang, L. M.; Gong, N. B.; Wu, L.; Wang, R. R.; Pu, J. X.; Li, X. L.; Huang, S. X.; Zheng, Y. T.; Li, R. T.; Lu, Y.; Zheng, Q. T.; Sun, H. D. *Org. Lett.* **2006**, *8*, 991–994.
(7) Shen, Y. C.; Lin, Y. C.; Chiang, M. Y.; Sheau, F. Y.; Cheng, Y. B.; Liao, C. C. *Org. Lett.* **2005**, *15*, 3307–3310.
(8) Pu, J. X.; Xiao, W. L.; Lu, Y.; Li, R. T.; Li, H. M.; Zhang, L.; Huang, S. X.; Li, X.; Zhao, Q. S.; Zheng, Q. T.; Sun, H. D. *Org. Lett.* **2005**, *22*, 5079–5082.
(9) Pu, J. X.; Li, R. T.; Xiao, W. L.; Gong, N. B.; Huang, S. X.; Lu, Y.; Zheng, Q. T.; Lou, L. G.; Sun, H. D. *Tetrahedron.* **2006**, *62*, 6073–6081.
(10) Tahtinen, P.; Bagno, A.; Klika, K. D.; Pihlaja, K. *J. Am. Chem.* **2003**, *125*, 4609–4618.
(11) Bagno, A. *Chem.−Eur. J.* **2001**, *7*, 1652–1661.
(12) Bagno, A.; Rastrelli, F.; Saielli, G. *Chem.−Eur. J.* **2006**, *12*, 5514–5525.
(13) Sedl, P. R.; Carneiro, J. W.; de, M.; Tostes, J. G. R.; Dias, J. F.; Pinto, P. S. S.; Costa, V. E. U.; Taft, C. A. *J. Mol. Struct.* **2002**, *579*, 101–107.
(14) Aiello, A.; Fattorusso, E.; Luciano, P.; Mangoni, A.; Menna, M. *Eur. J. Org. Chem.* **2005**, *23*, 5024–5030.
(15) Sebag, A. B.; Friel, C. J.; Hanson, R. N.; Forsyth, D. A. *J. Org. Chem.* **2000**, *65*, 7902–7912.
(16) Liu, D. Z.; Wang, F.; Liao, T. G.; Tang, J. G.; Steglich, W.; Zhu, H. J.; Liu, J. K. *Org. Lett.* **2006**, *8*, 5749–5752.
(17) Sica, D.; Musumeci, D.; Zollo, F.; Marino, S. De. *Eur. J. Org. Chem.* **2001**, *19*, 3731–3739.
(18) Fisch, M. J.; Trucks, G. W.; Schlegel, H. B.; Scuseris, G. E.; Robb, M. A.; Cheeseman, J. R.; Montgomery, J. A., Vreven, T., Kudin, K. N., Burant, J. C., Millam, J. M., Iyengar, S. S., Tomasi, J., Barone, V., Mennucci, B., Cossi, M., Scalmani, G., Rega, N., Petersson, G. A., Nakatsuji, H., Hada, M., Ehara, M., Toyota, K., Fukuda, R., Hasegawa, J., Ishida, M., Nakajima, T., Honda, Y., Kitao, O., Nakai, H., Klene, M., Li, X., Knox, J. E., Hratchian, H. P., Cross, J. B., Adamo, C., Jaramillo, J., Gomperts, R., Stratmann, R. E., Yazyev, O., Austin, A. J., Cammi, R., Pomelli, C., Ochterski, J. W., Ayala, P. Y., Morokuma, K., Voth, G. A., Salvador, P., Dannenberg, J. J., Zakrzewski, V. G., Dapprich, S., Daniels, A. D., Strain, M. C., Farkas, O., Malick, D. K., Rabuck, A. D., Raghavachari, K., Foresman, J. B., Ortiz, J. V., Cui, Q., Baboul, A. G., Clifford, S., Cioslowski, J., Stefanov, B. B., Liu, G., Liashenko, A., Piskorz, P., Komaromi, I., Martin, R. L., Fox, D. J., Keith, T., Al-Laham, M. A., Peng, C. Y., Nanayakkara, A., Chalacombe, M., Gill, P. M. W., Johnson, B. G., Chen, W., Wong, M. W., Gonzalez, C., Pople, J. A. *Gaussian 03 (revision B.05)*; Gaussian: Pittsburgh, PA, 2003.
(19) Monks, A.; Scudiero, D.; Skehan, P.; Shoemaker, R.; Paull, K.; Vistica, D.; Hose, C.; Langley, J.; Cronise, P.; Vaigro-Wolff, A.; Gray-Goodrich, M.; Campbell, H.; Mayo, J.; Boyd, M. *J. Natl. Cancer Inst.* **1991**, *83*, 757–766.

NP070247A